J Mater Sci (2009) 44:379–384
DOI 10.1007/s10853-008-3150-8

Study on the interaction between a dislocation and impurities in KCl:Sr^{2+} single crystals by the Blaha effect—Part IV influence of heat treatment on dislocation density

Y. Kohzuki

Received: 25 September 2008 / Accepted: 1 December 2008 / Published online: 20 December 2008

Abstract Strain-rate cycling tests associated with ultrasonic oscillation were carried out at 80–239 K for two kinds of KCl:Sr^{2+} (0.05 mol.% in the melt) single crystals: one is a quenched specimen and the other an annealed one. In this study, it was found that the density of moving dislocation is not influenced by the heat treatment. Furthermore, the increase in forest dislocation density for the annealed specimen seemed to be remarkable under the compression test, compared with that for the quenched specimen. As a result, the strain-hardening rate increased and the extent of plastic deformation region became short at a given temperature by annealing the quenched specimens. The investigation concerning forest dislocation density was conducted on the basis of the $\Delta(\Delta\tau'/\Delta \ln \dot{\varepsilon})/\Delta\varepsilon$, which will represent the variation of the strain-rate sensitivity due to dislocation cuttings with shear strain.

Introduction

It has so far been reported [1–5] that the information on the interaction between a moving dislocation and impurities is obtained on the basis of the relative curve of strain-rate sensitivity (SRS) and stress decrement due to ultrasonic oscillation. The curve is considered to reflect the influence of ultrasonic oscillation on the dislocation motion on the slip plane containing many impurities and a few forest dislocations [1, 2].

When alkali halide crystals are doped with divalent ions, the ions are expected to be paired with positive ion vacancies. The pairs are termed I–V dipoles. If the I–V dipoles in KCl:Sr^{2+} single crystals aggregate by heat treatment, the change in the state of a small amount of impurities strongly influences the resistance to movement of a dislocation [6]. Therefore, various deformation characteristics will be changed. In parts I [7] and II [8] of this series, it was found that the Fleischer's model [9], taking account of the Friedel relation [10], is suitable for the interaction between a dislocation and the impurity in the crystals but not for the annealed ones. This was examined mainly on the basis of the dependence of SRS due to the impurities on temperature. In part III [11], the influence of the heat treatment on the various characteristics (the force acted on the dislocation and the bending angle of dislocation by the impurity, dislocation velocity-effective stress exponent, etc.) was described from the relative curve of SRS and stress decrement due to the oscillation. In this study, it is investigated whether the density of the dislocation is changed by the heat treatment under the compression test. This is examined from the relation between SRS and stress decrement carried out so far.

Experimental procedure

Two kinds of KCl:Sr^{2+} (0.05 mol.% in the melt) single crystals, which are the size of about $5 \times 5 \times 15$ mm^3, were deformed at 80–239 K by compression along the <100> axis and ultrasonic oscillatory stress was applied by a resonator in the same direction as the compression. One kind of the specimens were obtained by following heat

Y. Kohzuki (✉)
Oshima National College of Maritime Technology, 1091-1 Komatsu, Suo-Oshima-cho, Oshima-gun, Yamaguchi 742-2193, Japan
e-mail: kouzuki@oshima-k.ac.jp

treatment. The specimens were cooled to room temperature at a rate of 40 K h^{-1} after keeping at 973 K for 24 h in order to reduce dislocation density. Further, the specimens were held at 673 K for 30 min and were cooled by water quenching in order to disperse the impurities immediately before the test. The specimen is termed the quenched specimen in this article. The other kind of specimens was obtained by keeping the quenched specimens at 370 K for 500 h and furnace cooling for the purpose of aggregating the impurities [12]. This is termed the annealed specimen in this article.

The stress drop due to superposition of oscillatory stress during plastic deformation is $\Delta\tau$, which increases with increasing the stress amplitude at a given temperature and shear strain. When the strain-rate cycling is carried out keeping the stress amplitude constant, the stress change due to the strain-rate cycling is $\Delta\tau'$. The strain-rate cycling tests associated with the oscillation have been described in the previous articles [2, 5].

Results and discussion

Influence of the heat treatment on moving dislocation density

When the thermally activated overcoming of the aggregates controls the dislocation velocity, the strain rate, $\dot{\varepsilon}$, is expressed by an Arrhenius-type equation [13]

$$\dot{\varepsilon} = \dot{\varepsilon}_0 \exp(-\Delta G/kT), \tag{1}$$

where $\dot{\varepsilon}_0$ is a frequency factor, ΔG is the change in Gibbs free energy of activation for the dislocation motion and kT has the usual meaning. The force, F, acting on the dislocation as a function of the distance, x, until the aggregate on the slip plane is given by

$$\begin{aligned} &F(x) = F_0(1 - |x|^n/a^n), \quad |x| < a \\ &(F(\pm a) = 0, F(0) = F_0), \end{aligned} \tag{2}$$

where square $F(x)$ is for the case of $n = \infty$, triangular $F(x)$ for $n = 1$ and parabolic $F(x)$ for $n = 2$ [14]. A square force-distance relation, a parabolic one and a triangular one are termed the SQ, the PA and the TR, respectively, in this article. Integrating Eq. 2 with respect to x, the Gibbs free energy is given by [15]

$$\Delta G = 2F_0 a\{n/(n+1)\}\{1 - (F/F_0)\}^{(n+1)/n} \tag{3}$$

The Gibbs free energy for the SQ is obtained from the Friedel relation [10]:

$$L = \left\{2L_0^2 E/(\tau b)\right\}^{1/3} \tag{4}$$

namely,

$$\Delta G = 2F_0 a\{1 - (F/F_0)\}, \tag{5}$$

where L_0 is the average spacing of impurities on the slip plane, E the line tension of the dislocations, τ the effective shear stress and b the magnitude of the Burgers vector. F and F_0 in Eq. 5 are expressed by using Eq. 4 as follows

$$F = \left(2L_0^2 E\right)^{1/3} b^{2/3} \tau^{2/3} \tag{6}$$

$$F_0 = \left(2L_0^2 E\right)^{1/3} b^{2/3} \tau_0^{2/3}, \tag{7}$$

where τ_0 is the effective shear stress at 0 K. When the F is zero, Eq. 3 can be transformed as the following:

$$\Delta G_0 = 2F_0 a\{n/(n+1)\} \tag{8}$$

Substituting of Eqs. 6–8 in Eq. 5, the Gibbs free energy for the SQ yields

$$\Delta G = \Delta G_0\left\{1 - (\tau/\tau_0)^{2/3}\right\} \tag{9}$$

Differentiating the substitutional equation of Eq. 9 in Eq. 1 with respect to the shear stress, we find

$$\partial \ln \dot{\varepsilon}/\partial\tau = \{2\Delta G_0/(3k)\}\left(\tau_{p0}^2 \tau_{p1}\right)^{-1/3}/T + \partial \ln \dot{\varepsilon}_0/\partial\tau, \tag{10}$$

where τ_0 and τ are replaced by τ_{p0} and τ_{p1}. τ_{p1} is considered to be the effective shear stress due to only one type of the impurities and τ_{p0} that due to the impurities without thermal activation when the dislocation moves forward with the help of oscillation [2]. $\partial \ln \dot{\varepsilon}/\partial\tau$ for the PA is expressed by [8]

$$\partial \ln \dot{\varepsilon}/\partial\tau = (\Delta G_0/k)\left\{\left(\tau_{p0}^2 \tau_{p1}\right)^{-2/3} - \tau_{p0}^{-2}\right\}^{1/2}/ T + \partial \ln \dot{\varepsilon}_0/\partial\tau \tag{11}$$

and that for the TR yields [8]

$$\partial \ln \dot{\varepsilon}/\partial\tau = \{4\Delta G_0/(3k)\}\left\{\left(\tau_{p0}^2 \tau_{p1}\right)^{-1/3} - \left(\tau_{p0}^{-4} \tau_{p1}\right)^{1/3}\right\}/ T + \partial \ln \dot{\varepsilon}_0/\partial\tau, \tag{12}$$

where τ_{p0} values for the three kinds of force–distance relations are re-tabulated in Table 1. The results of calculations for Eqs. 10–12 are shown in Fig. 1a–c in which the $\partial \ln \dot{\varepsilon}/\partial\tau$ is represented by $(\Delta \ln \dot{\varepsilon}/\Delta\tau')_p$. The $(\Delta\tau'/\Delta \ln \dot{\varepsilon})_p$, which is given by the difference between SRS at first plateau place and at second one on the relative curve of SRS and stress decrement, is assumed to be the SRS due to the impurities [3–5]. Accordingly, $\partial \ln \dot{\varepsilon}_0/\partial\tau$ in Eqs. 10–12 can be represented by $\Delta \ln \dot{\varepsilon}_0/\Delta\tau'$. The $\Delta \ln \dot{\varepsilon}_0/\Delta\tau'$ corresponds to the value at which the solid lines intersect the ordinate in these figures. The results are given in Table 1. The $\Delta \ln \dot{\varepsilon}_0/\Delta\tau'$ is expressed by [16]

Table 1 Values of τ_{p0} and $\Delta \ln \dot{\varepsilon}_0/\Delta\tau'$ for the three force–distance relations between a dislocation and the aggregate in the annealed specimen

Force–distance relation	τ_{p0} (MPa)	$\Delta \ln \dot{\varepsilon}_0/\Delta\tau'$ (MPa^{-1})
SQ	2.17	6.80
PA	3.28	10.46
TR	4.53	10.57

$$\Delta \ln \dot{\varepsilon}_0/\Delta\tau' = (\Delta \ln \rho/\Delta\tau') + 2/(3\tau_{p0}), \quad (13)$$

where ρ is the density of mobile dislocation. Substituting the values of $\Delta \ln \dot{\varepsilon}_0/\Delta\tau'$ and τ_{p0} into Eq. 13, $(\Delta\rho/\Delta\tau')$ can be obtained. These values for the three force–distance relations are given in Table 2. The values of $(\Delta\rho/\Delta\tau')$ are within stage II of stress–strain curve, because the $(\Delta\tau'/\Delta \ln \dot{\varepsilon})_p$ values in Fig. 1a–c are obtained on the basis of the relative curve of SRS and stress decrement in stage II. Although the values of $(\Delta \ln \dot{\varepsilon}/\Delta\tau')_p$ are slightly scattering as shown in Fig. 1a–c, $(\Delta\rho/\Delta\tau')$ for the annealed specimen seems to be less than 3.38 cm^{-2} MPa^{-1}. From Table 2, it is difficult to discriminate the difference in $(\Delta\rho/\Delta\tau')$ among the three. On the other hand, that for the quenched specimen was 0.79 cm^{-2} MPa^{-1} [16]. Therefore, it is considered that the density of moving dislocation is not influenced by the heat treatment in this study.

Strain-rate sensitivity at second plateau place on the relative curve of strain-rate sensitivity and stress decrement

There are two bending points and two plateau places, and SRS decreases with stress decrement between two bending points on the relative curve of SRS and stress decrement at a given shear strain and temperature for the two kinds of specimens [3]. However, it is occasionally observed that the SRS increases with stress decrement at the second plateau place on the curve in stage I for the annealed specimen. Figure 2 shows the phenomenon. The SRS at second plateau place on the curve is considered to be due to dislocation cuttings [2]. As for the quenched specimen, the same phenomenon as Fig. 2 does not appear. We investigate the relation between temperature and the variation of SRS at the second plateau place on the relative curve of SRS and stress decrement with shear strain, $\Delta(\Delta\tau'/\Delta \ln \dot{\varepsilon})/\Delta\varepsilon$, in the different plastic deformation regions of stress–strain curve for the two kinds of specimens. The $\Delta(\Delta\tau'/\Delta \ln \dot{\varepsilon})/\Delta\varepsilon$ seems to be the variation of the SRS due to dislocation cuttings with shear strain [17]. Three-stage strain hardening is obtained for KCl [18, 19] and is also observed for KCl:Sr^{2+} (0.05 mol.% in the melt). The size of specimens used at the following research in this section is within $(5 \pm 1) \times (5 \pm 1) \times (15 \pm 1)$ mm^3. Because, it has been reported that the height-width of specimens determines the shape of the work-hardening

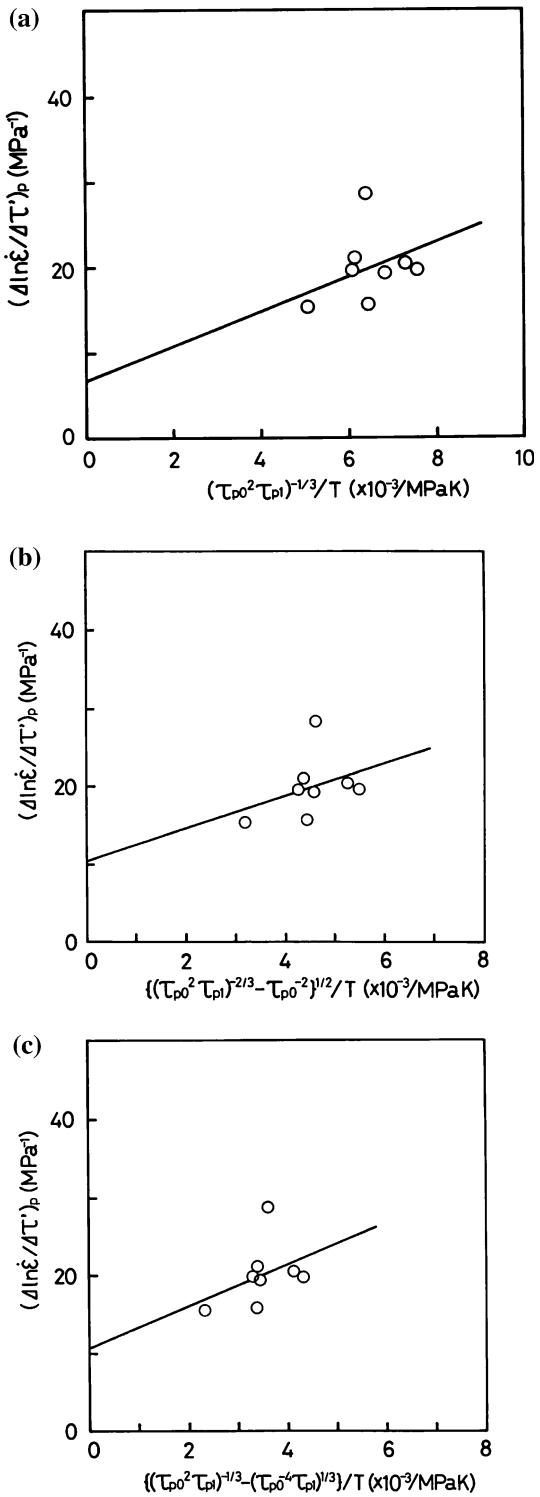

Fig. 1 Linear plots of **a** Equation 10 for the SQ, **b** Equation 11 for the PA [8] and **c** Equation 12 for the TR [8]. (○): $(\Delta \ln \dot{\varepsilon}/\Delta\tau')_p$ for the annealed specimen

Table 2 Values of $\Delta\rho/\Delta\tau'$ for the three force–distance relations between a dislocation and the aggregate in the annealed specimen

Force–distance relation	$\Delta\rho/\Delta\tau'$ (cm^{-2} MPa^{-1})
SQ	0.07
PA	2.85
TR	3.38

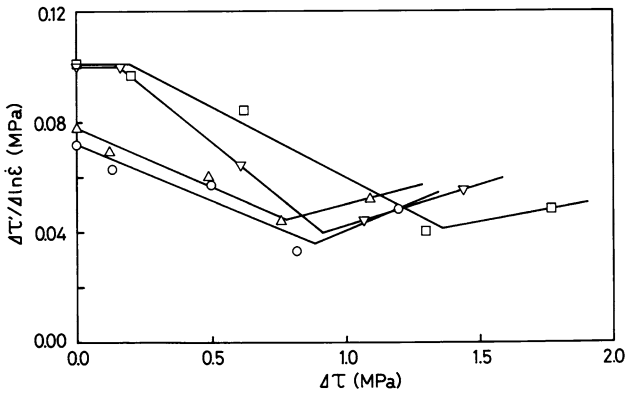

Fig. 2 Relationship between the strain-rate sensitivity and the stress decrement for the annealed specimen at various conditions: (□) 183 K and $\varepsilon = 7\%$, (▽) 187 K and $\varepsilon = 6\%$, (○) 201 K and $\varepsilon = 6\%$, (△) 201 K and $\varepsilon = 9\%$

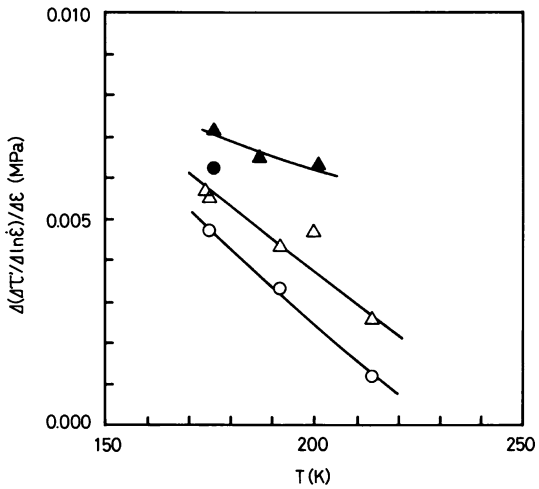

Fig. 3 Dependence of $\Delta(\Delta\tau'/\Delta\ln\dot{\varepsilon})/\Delta\varepsilon$ on the temperature in the different plastic deformation regions: (○) for the quenched specimen and (●) for the annealed specimen in stage I; (△) for the quenched specimen and (▲) for the annealed specimen in stage II

curve in the compression at a constant strain rate and temperature for CaF_2 single crystals [20] and besides glide geometry is directly related to the shape and size of KCl crystals [21]. In Fig. 3, the relations of temperature and $\Delta(\Delta\tau'/\Delta\ln\dot{\varepsilon})/\Delta\varepsilon$ in stage I and in stage II are represented by a circle and a triangle, respectively. The open symbols correspond to that for the quenched specimen and the solid ones that for the annealed specimen. The curves in Fig. 3 are to guide the reader's eye. Unfortunately, the $\Delta(\Delta\tau'/\Delta\ln\dot{\varepsilon})/\Delta\varepsilon$ could not be obtained at low temperature. The same two phenomena as described for KCl:Li^+ (0.5 mol.% in the melt) and KCl:Na^+ (0.5 mol.% in the melt) in the previous article [17] are also observed for both the quenched specimen and the annealed specimen in Fig. 3. That is, the first phenomenon is that the $\Delta(\Delta\tau'/\Delta\ln\dot{\varepsilon})/\Delta\varepsilon$ in stage II is obviously larger than that in stage I at a given temperature. The other phenomenon is that the $\Delta(\Delta\tau'/\Delta\ln\dot{\varepsilon})/\Delta\varepsilon$ in stage I and in stage II increases with decreasing temperature. Figure 3 also shows that the $\Delta(\Delta\tau'/\Delta\ln\dot{\varepsilon})/\Delta\varepsilon$ for the annealed specimens is considerably large in contrast to that for the quenched specimens in the two stages at the temperature. This may result from a rapid increase in forest dislocation density with shear strain in the annealed specimen. Accordingly, the increase in that in the annealed specimen seems to be remarkable in the two stages under the compression test, compared with that in the quenched specimen. According to Michalak [22] some dislocation cutting process becomes an important hardening mechanism and the strain-hardening increases. If the consideration about forest dislocation density for the two kinds of specimens is accurate, it is expected that a strain-hardening rate, $d\tau/d\varepsilon$, for the annealed specimen is larger than that for the quenched specimen at a given temperature and shear strain.

When the whole crystal is filled with primary dislocation dipoles and multipoles, stage I ends and the stage II, which is characterized by the onset of glide on oblique systems, follows. Afterwards, the stage III, which is probably associated with the cross glide of screw dislocation around obstacles, ensues in the process of plastic deformation [23]. Accordingly, it will be also expected that the extent of stage I and stage II for the annealed specimen is shorter than that for the quenched specimen at a given temperature.

The relation between strain-hardening rate and temperature for the two kinds of specimens is shown in Fig. 4a for stage I and b for stage II. The value of strain-hardening rate in stage II is about two times larger than that in stage I at a given temperature for both the specimens. Furthermore, the strain-hardening rate for the annealed specimen is obviously large as against that for the quenched specimen in the two stages as can be seen from Fig. 4a and b. We then investigate the extent of stage I and stage II. However, the difference between the extent of stage I for the two kinds of specimens could not be found out within the temperature. The extent of stage II for the quenched specimen could not also be compared with that for the annealed specimen, because most of the specimens were fractured within stage II by the compression test. Then, we attempt to investigate the extent between shear strains of yield point and of fractured point, i.e. plastic deformation region, at various

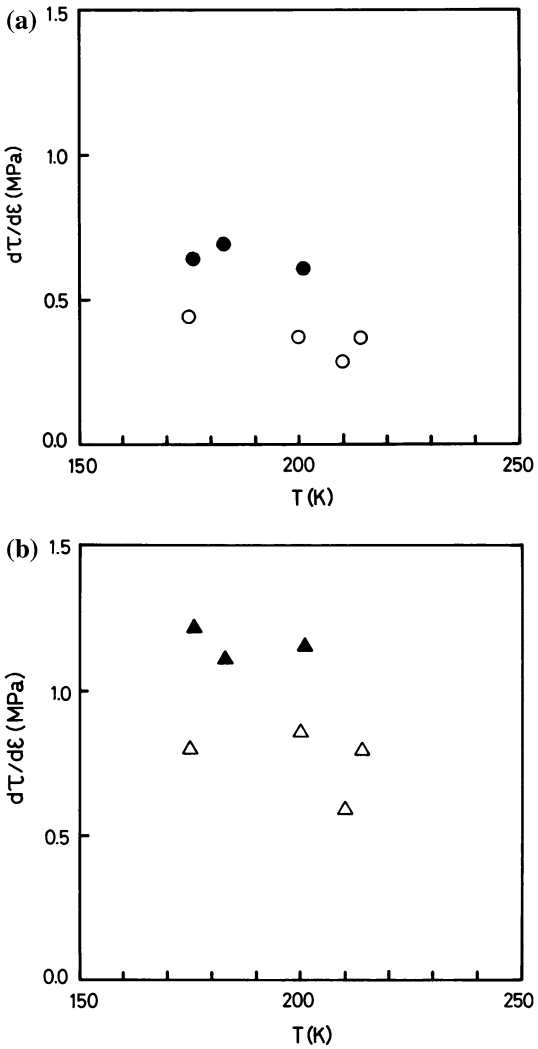

Fig. 4 Dependence of the strain-hardening rate on the temperature in the different plastic deformation regions: **a** (○) for the quenched specimen and (●) for the annealed specimen in stage I; **b** (△) for the quenched specimen and (▲) for the annealed specimen in stage II

temperatures. The result of the extent of plastic deformation region is shown in Fig. 5. The open circles and the solid ones correspond to that for the quenched specimen and for the annealed specimen, respectively. The extent of it tends to be large with increasing temperature for both the specimens. Figure 5 also shows that the extent of that for the annealed specimen seems to be shorter than that for the quenched specimen at a given temperature. Consequently, it is clear that the increase in forest dislocation density in the annealed specimen is remarkable in contrast to that in the quenched specimen under the compression test. This may be attributed to the phenomenon that a small amount of the much larger aggregates than trimers, which are contained in the annealed specimen, contribute to the increase in forest dislocation density.

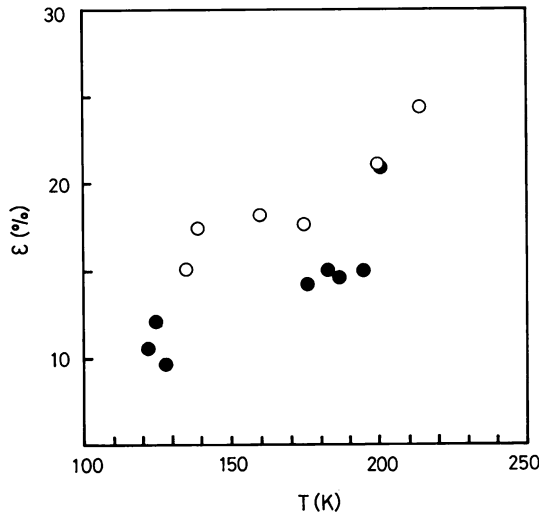

Fig. 5 Dependence of the extent of plastic deformation region on the temperature for both the specimens: (○) for the quenched specimen and (●) for the annealed specimen

Conclusions

The following conclusions were derived from the results and discussion based on the relative curve of SRS and stress decrement due to the oscillation:

1. The increase in mobile dislocation density with the stress change, $(\Delta\rho/\Delta\tau')$, seems to be less than 3.38 cm^{-2} MPa^{-1} for the annealed specimen and is not influenced by the heat treatment in this study.
2. The increase in forest dislocation density with shear strain for the annealed specimen is remarkable in both stage I and stage II of stress–strain curve at 170–220 K under the compression test, compared with that for the quenched specimen. As a proof of it, the following two experimental results are obtained. First, the strain-hardening rate for the annealed specimen is obviously larger than that for the quenched specimen in the two stages within the temperature. Second, the extent of plastic deformation region becomes short at a given temperature by annealing the quenched specimen.

References

1. Ohgaku T, Takeuchi N (1992) Phys Status Solidi (a) 134:397
2. Kohzuki Y, Ohgaku T, Takeuchi N (1993) J Mater Sci 28:3612. doi:10.1007/BF01159844
3. Kohzuki Y, Ohgaku T, Takeuchi N (1993) J Mater Sci 28:6329. doi:10.1007/BF01352192
4. Kohzuki Y, Ohgaku T, Takeuchi N (1995) J Mater Sci 30:101. doi:10.1007/BF00352137
5. Kohzuki Y (1998) J Mater Sci 33:5613. doi:10.1023/A:1004468332474
6. Dryden JS, Morimoto S, Cook JS (1965) Philos Mag 12:379

7. Kohzuki Y (2000) J Mater Sci 35:3397. doi:10.1023/A:1004889203796
8. Kohzuki Y, Ohgaku T (2001) J Mater Sci 36:923. doi:10.1023/A:1004807403566
9. Fleischer RL (1962) J Appl Phys 33:3504
10. Friedel J (1964) Dislocations. Pergamon Press, Oxford, p 224
11. Kohzuki Y, Ohgaku T (2004) J Mater Sci 39:107. doi:10.1023/B:JMSC.0000007733.42000.39
12. Cook JS, Dryden JS (1962) Proc Phys Soc 80:479
13. Christian JW, Masters BC (1964) Proc R Soc A281:240
14. Foreman AJE, Makin MJ (1966) Philos Mag 14:911
15. Sumino K (1972) Jpn Inst Metals 11:31 (in Japanese)
16. Kohzuki Y (2003) J Mater Sci 38:953. doi:10.1023/A:1022373124795
17. Kohzuki Y (2000) J Mater Sci 35:2273. doi:10.1023/A:1004735128091
18. Alden TH (1964) Trans Met Soc AIME 230:649
19. Davis LA, Gordon RB (1969) J Appl Phys 40:4507
20. Evans AG, Pratt PL (1970) Philos Mag 21:951
21. Suszyńska M (1974) Kristall Technik 9:1199
22. Michalak JT (1965) Acta Metall 13:213
23. Sprackling MT (1976) In: Alper AM, Margrave JL, Nowick AS (eds) The plastic deformation of simple ionic crystals. Academic Press, London, p 203